Volume 60
Number 88
14 November 2024
Pages 12777–12938

ChemComm

Chemical Communications

rsc.li/chemcomm

ISSN 1359-7345

ROYAL SOCIETY OF CHEMISTRY

COMMUNICATION

Xujun Qiu, Stefan Bräse *et al.*

A simple method to modulate the selectivity of aryl azide photolysis using cucurbit[8]uril

60 YEARS ANNIVERSARY

ChemComm

COMMUNICATION

View Article Online
View Journal | View Issue

Cite this: *Chem. Commun.*, 2024, **60**, 12852

Received 18th August 2024,
Accepted 2nd October 2024

DOI: 10.1039/d4cc04209c

rsc.li/chemcomm

A simple method to modulate the selectivity of aryl azide photolysis using cucurbit[8]uril†

Xujun Qiu,*[a] Qianyu Cai,[a] Eric Pohl,[b] André Jung,[c] Haopu Su,[a] Olaf Fuhr,[de] Ute Schepers[ab] and Stefan Bräse*[ac]

Photolysis of aryl azides typically involves multiple reaction pathways. This study designed and synthesized an aryl azide rotamer with two conformations. In aqueous media, its photolysis yields two main products. However, when stabilized in one conformation within the cucurbit[8]uril (CB8) host, the photoreaction selectively produces a single product.

Inspired by enzyme pockets, which use reversible noncovalent interactions to preorganize substrate conformation, specific reaction pathways can be achieved.[1] Chemical reactions in supramolecular hosts, specifically synthetic hosts such as macrocyclic molecules,[2–4] cages,[5–7] and capsules,[8–10] have garnered increasing interest. The confined spaces within these supramolecular hosts act as micro-reaction chambers, stabilizing guest molecules and enabling modulated reactions that pave the way for novel chemical processes.[11]

Among macrocyclic supramolecular hosts, cucurbit[*n*]urils (CBn) are pumpkin-shaped molecules composed of repeating glycoluril units bridged by methylene groups.[12] With their hydrophobic inner cavities and polar portals, CBn can capture cationic guests with high binding affinity.[13] They have shown potential as reaction chambers for modulating various chemical reactions,[14–16] such as photodimerization,[17–19] the Diels–Alder reaction,[20–22] 1,3-dipolar cycloaddition,[23–25] and more.[26–34]

Organic azides feature diverse reactivities that can be harnessed under various reaction conditions.[35] Photolysis of aryl azides provides a convenient approach to synthesize carbazole and carboline derivatives by intramolecular C–H amination. However, the highly reactive singlet nitrene generated during photolysis often leads to multiple reaction pathways,[36] potentially resulting in undesired byproducts.

Our previous studies demonstrated the potential to modulate aryl azide photolysis using CB7 for selective intramolecular C–H amination,[37] and CB8 to facilitate photolysis of a paracyclophane (PCP) azide.[38] However, the latter showed poor selectivity likely due to the flexible rotation of the pyridinium ring within the CB8 cavity, leading to multiple reaction pathways.

To test this hypothesis, we designed a new PCP aryl azide (**1**), with a quinolinium moiety (Scheme 1). Due to the steric effects of the quinolinium, azide **1** exists as rotamers. Photolysis of **1** in aqueous media yields two C–H aminated products, **2** and **3**, corresponding to the two rotamer conformations. However, encapsulating aryl azide **1** in CB8 restricts quinolinium rotation, forming a stable **1**·CB8 complex. As a result, photolysis produced only one C–H amination product, **3**·CB8.

The synthetic details of rotamer **1** are given in ESI† (Fig. S1–S8). The photoreaction of **1** was initially studied in an aqueous media by ^{1}H NMR. As shown in Fig. S9 (ESI†), a different NMR spectrum was observed after the photoreaction. Liquid chromatography-mass spectrometry (LC-MS) was utilized to determine the molecular weight of the products, as presented in Fig. S10 (ESI†). The LC-MS spectra suggest two main species were formed with the molecular mass 363.28 g mol^{-1} and 363.29 g mol^{-1}, which are likely the C–H aminated products, compared to the aryl azide **1** with a molecular mass of 391.32 g mol^{-1}.

To monitor the reaction process, UV-vis and emission spectra were recorded (Fig. S11, ESI†), revealing completion after approximately 400s. Two products were further seperated using preparative high-performance chromatography (prep HPLC). Single crystals were obtained to unveil the structures (Fig. 1

[a] *Institute of Organic Chemistry (IOC), Karlsruhe Institute of Technology (KIT), Kaiserstraße 12, 76131 Karlsruhe, Germany. E-mail: xujun.qiu@kit.edu, braese@kit.edu*
[b] *Institute of Functional Interfaces (IFG), Karlsruhe Institute of Technology (KIT), Kaiserstraße 12, 76131 Karlsruhe, Germany*
[c] *Institute of Biological and Chemical Systems – Functional Molecular Systems (IBCS-FMS), Karlsruhe Institute of Technology (KIT), Kaiserstraße 12, 76131 Karlsruhe, Germany*
[d] *Institute of Nanotechnology (INT), Karlsruhe Institute of Technology (KIT), Kaiserstraße 12, 76131 Karlsruhe, Germany*
[e] *Karlsruhe Nano Micro Facility (KNMFi), Karlsruhe Institute of Technology (KIT), Kaiserstraße 12, 76131 Karlsruhe, Germany*

† Electronic supplementary information (ESI) available. CCDC 2377053–2377055. For ESI and crystallographic data in CIF or other electronic format see DOI: https://doi.org/10.1039/d4cc04209c

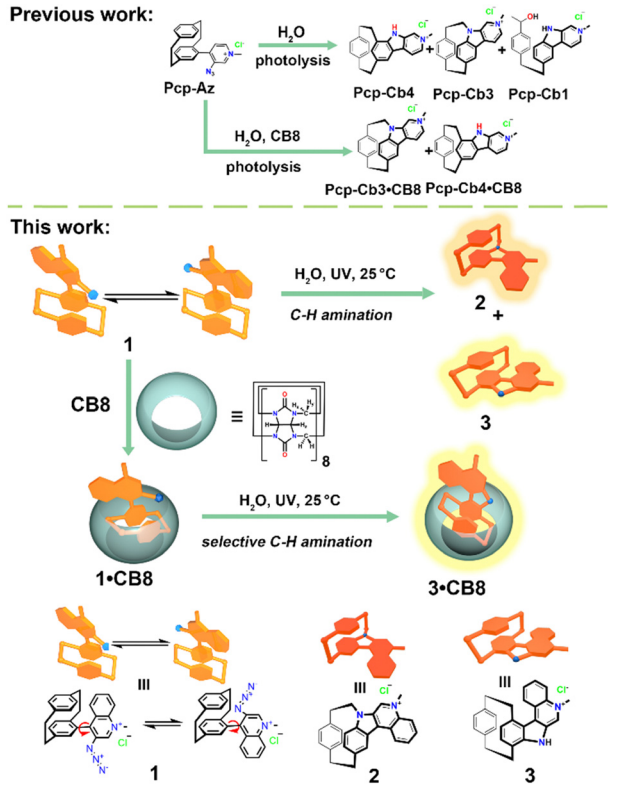

Scheme 1 Schematic illustration of stabilizing and regulating the photoreaction outcome aryl azide **1** within cucurbit[8]uril.

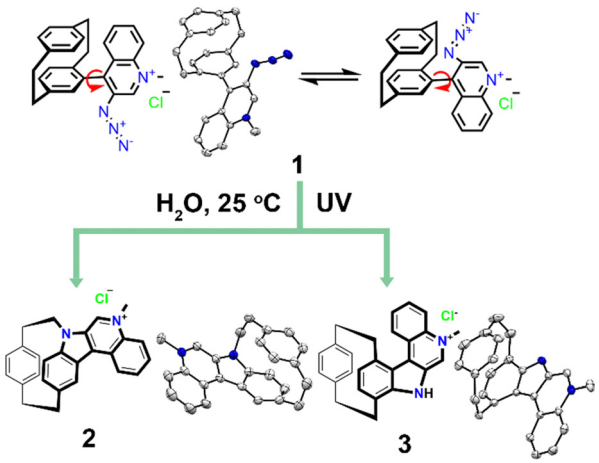

Fig. 1 Chemical structures of rotamer **1** and the photolysis products **2** and **3**.

and Fig. S12, S13 and Tables S1, S2, ESI†), which reveal a C–H aminated and intramolecular rearranged product **2** and a direct C–H aminated product **3**. The NMR characterization can be seen in Fig. S14–S17 (ESI†). Unlike previously designed PCP-azide, which also yields a hydrolyzed product,[38] aryl azide **1** benefits from a larger aromatic conjugation. This gives the possibility of aggregation in water (see crystal structures in Fig. S18 and Table S3, ESI†), thus diminishing the chances of being attacked by water nucleophiles. Consequently, only two products were obtained.

To investigate the photolysis of aryl azide **1** within the CB8 cavity, we first studied the host–guest interactions using ^{1}H NMR spectroscopy. As depicted in Fig. 2a-(ii) and Fig. S19 and S20 (ESI†), the introduction of an equimolar amount of CB8 to the solution of **1** causes significant upfield shifts in the signals from the PCP moiety, indicating deep encapsulation of the PCP moiety within the CB8 cavity. Additionally, deformation of CB8 was observed, as evidenced by the split signals H_x and H_y from CB8, similar to other reported PCP molecules.[38–40] Notably, the split signals from rotamer **1** show only one set, suggesting that **1** stabilizes in one single conformation.

The formation of 1 : 1 host–guest complex between aryl azide **1** and CB8 was further confirmed by electrospray ionization mass spectrometry (ESI-MS) (Fig. S21, ESI†), where a mass-to-charge ration (m/z) of 1720.5872 for [**1** + CB8-Cl]$^+$ was obtained. The binding behavior of **1** with CB8 was investigated using UV-titration. As depicted in Fig. 2b, the addition of CB8 to the solution of **1** resulted in a gradual decrease in absorbance, leading to isosbestic points. The absorbance change at 398 nm as a function of CB8 concentration is plotted in Fig. 2c. A least-squares fitting with a direct binding model (DBA) yielded a binding constant of $(1.67 \pm 0.13) \times 10^7$ M^{-1} (Fig. S22, ESI†), indicating strong stabilization of the **1** in the CB8 cavity.

Photolysis of **1** within the CB8 cavity was performed under the same condition as for **1** in water. After irradiation, the ^{1}H NMR signals (Fig. 2a-(iii) and Fig. S23, S24, ESI†) showed only one species, **3**·CB8, indicating selective conversion. The photoreaction of **1** within the CB8 was monitored using UV-vis and emission spectra (Fig. S25, ESI†), revealing that the reaction was completed within 420s. Upon the introducing of a strong–binding guest, memantine hydrochloride, to the reaction mixture, **3** was expelled from the CB8 cavity, resulting in the formation of unbound **3** (Fig. 2a-(iv) and Fig. S26, S27, ESI†). The binding constant of **3** with CB8 was determined as $(1.02 \pm 0.14) \times 10^8$ M^{-1} (Fig. S28, ESI†).

To further elucidate the rotational barrier involved in the formation of carboline **3** within and without the CB8 cavity, we performed a relaxed potential energy surface (PES) scan for the dihedral angle (D) of C154–C155–C161–C162 in **1**·CB8 complex (Fig. S29, ESI†) and its corresponding angle C10–C11–C17–C18 in **1** (Fig. S30, ESI†). Geometry optimization of **1**·CB8 at 6-31G(d,p)/B3LYP/D3 level gave the starting value of 30° for D, which was adopted by **1** for comparison purpose. As depicted in Fig. 3, two stable conformers, **A** with D at 50° and **C** at 230°, were confirmed with the minima of relative energy, −1.7 kcal mol^{-1} and −1.2 kcal mol^{-1}. This consistent with the NMR observations for two rotamers (Fig. 2a-(i)). The 0.5 kcal mol^{-1} energy difference between **A** and **C** accounts for the non − 1 : 1 ratio in the NMR integrals. Energy maxima for conformer **B** and **D** occur at 170° and 0° along the scanning coordinate, with small 50° difference from the nearest minima, offering key insights to the reaction coordinate.

For **1** hosted in CB8 cavity, two energy minima corresponding to conformers **A′** and **C′** are observed, similar to the case without CB8. However, within the cavity, **A′** and **C′** are distorted, with D values of 30° and 250°, respectively. Energetically, **C′** is 5.2 kcal mol^{-1} higher than **A′**, leading to its lower or negligible

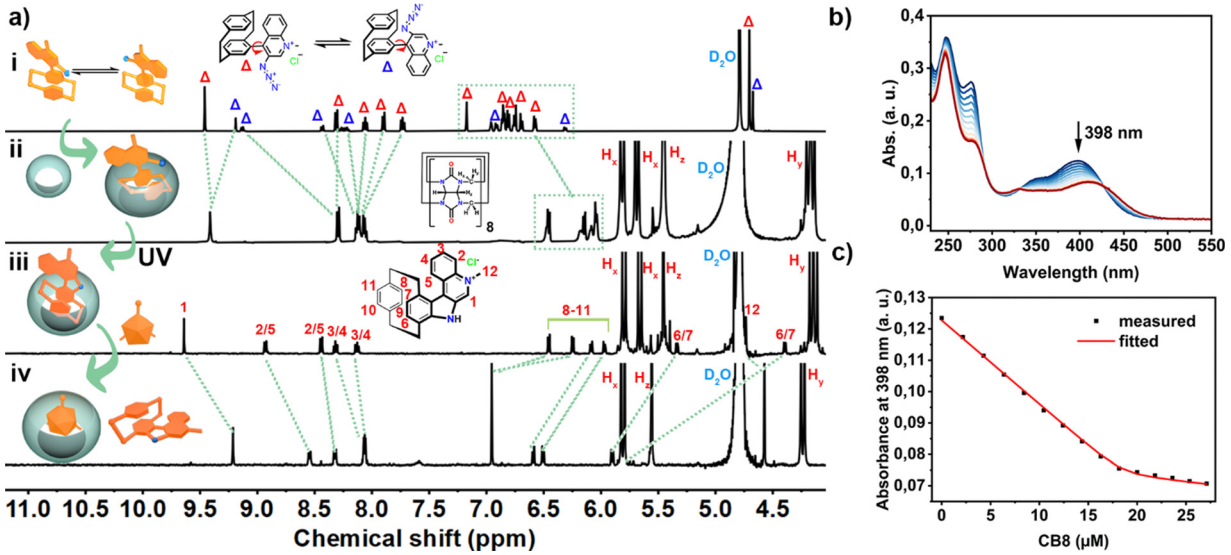

Fig. 2 (a) Partial ^{1}H NMR spectra of (i) **1** (0.5 mM), (ii) **1**·CB8 (1 : 1, 0.5 mM), (iii) **3**·CB8 (1 : 1, 0.5 mM), and (iv) **3** (0.5 mM) in D_2O; (b) UV-vis titration spectra of **1** (**1** = 20 μM) upon addition of CB8 (CB8 = 0–27.1 μM) in an aqueous solution at 298 K; (c) least-square curve fitting of the UV absorbance changes at 398 nm against the concentration of CB8 for binding constant between **1** and CB8 determining.

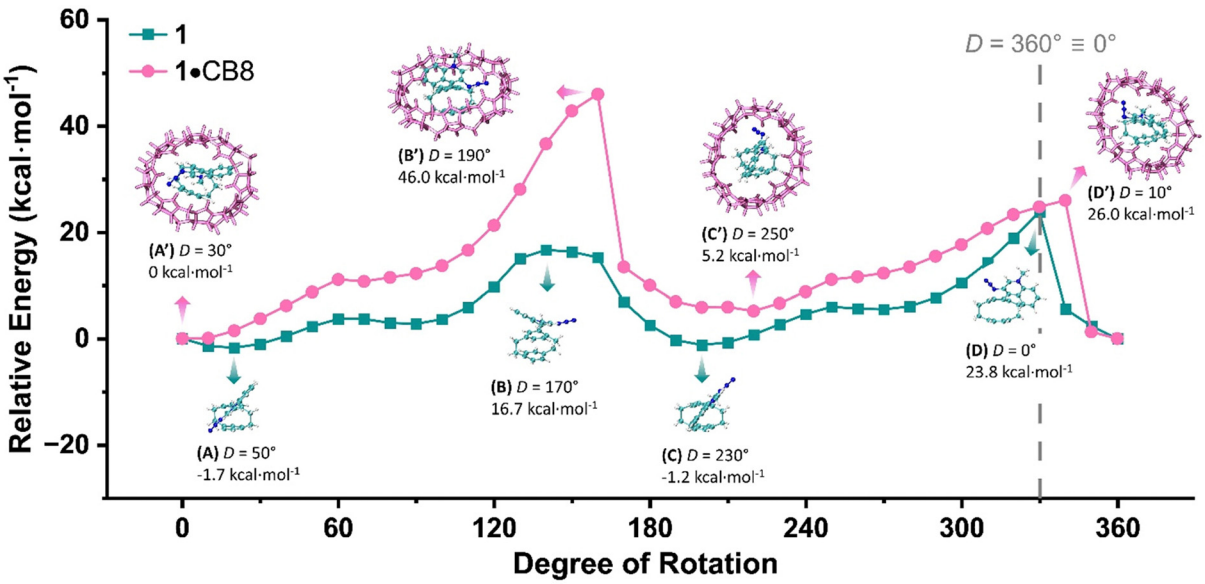

Fig. 3 Potential energy surface (PES) scan for dihedral angle of C154–C155–C161–C162 in **1**·CB8 and C10–C11–C17–C18 in **1** starting from 30°.

occurrence, consistent with the NMR analysis (Fig. 2a-(ii)). The rotational barrier from **A**′ to **B**′ is as high as 46 kcal mol^{-1}, while the counterclockwise rotation from **A**′ to **D**′ requires only 26 kcal mol^{-1}. This 20 kcal mol^{-1} energy difference contributes to the observed selectivity in the photolysis of **1** within the CB8 cavity.

In conclusion, we developed a novel strategy to control the photolysis of aryl azide rotamers using the supramolecular host CB8. The photoreaction of the rotamers was tuned to yield two C–H aminated products corresponding to the two rotamer conformations. Encapsulation within the CB8 cavity stabilized a single rotamer conformation, resulting in the exclusive formation of one product upon photolysis. Potential energy surface (PES) analysis elucidates the rotational barrier associated with the formation of this product within CB8. This work will be of interest for producing desired bioactive carbolines,[41] utilizing supramolecular hosts to modulate molecular conformations and the reaction pathways.

The authors acknowledge support from China Scholarship Council (CSC grant: 202010190002) and Prof. H.-A. Wagenknecht (IOC, KIT) for access to photophysics equipment. Support from the state Baden-Württemberg through bwHPC and German Research Foundation (DFG), grant no INST 40/575-1 FUGG (JUSTUS 2 cluster) and 3DMM2O – EXC-2082/1–390761711, is also greatly acknowledged.

Data availability

Data for this article, including NMR, IR are available at Chemotion Repository at **https://www.chemotion-repository.net/welcome** *via* DOI given in the ESI.†

Conflicts of interest

There are no conflicts to declare.

References

1 K.-Y. Wang, J. Zhang, Y.-C. Hsu, H. Lin, Z. Han, J. Pang, Z. Yang, R.-R. Liang, W. Shi and H.-C. Zhou, *Chem. Rev.*, 2023, **123**, 5347–5420.
2 J. Yu, D. Qi and J. Li, *Commun. Chem.*, 2020, **3**, 189.
3 L. A. Fontana, M. P. Almeida, A. F. P. Alcântara, V. H. Rigolin, M. A. Ribeiro, W. P. Barros and J. D. Megiatto, *Nat. Commun.*, 2020, **11**, 6370.
4 C. Wang, L. Xu, Z. Jia and T.-P. Loh, *Chin. Chem. Lett.*, 2024, **35**, 109075.
5 E. G. Percástegui, T. K. Ronson and J. R. Nitschke, *Chem. Rev.*, 2020, **120**, 13480–13544.
6 R. Ham, C. J. Nielsen, S. Pullen and J. N. H. Reek, *Chem. Rev.*, 2023, **123**, 5225–5261.
7 T. K. Piskorz, V. Martí-Centelles, R. L. Spicer, F. Duarte and P. J. Lusby, *Chem. Sci.*, 2023, **14**, 11300–11331.
8 Q. Zhang, L. Catti and K. Tiefenbacher, *Acc. Chem. Res.*, 2018, **51**, 2107–2114.
9 N. Borlinghaus, J. Kaschel, J. Klee, V. Haller, J. Schetterl, S. Heitz, T. Lindner, J. D. Dietrich, W. M. Braje and A. Jolit, *J. Org. Chem.*, 2021, **86**, 1357–1370.
10 V. Ramamurthy, *Chem. Commun.*, 2022, **58**, 6571–6585.
11 M. Morimoto, S. M. Bierschenk, K. T. Xia, R. G. Bergman, K. N. Raymond and F. D. Toste, *Nat. Catal.*, 2020, **3**, 969–984.
12 W. A. Freeman, W. L. Mock and N. Y. Shih, *J. Am. Chem. Soc.*, 1981, **103**, 7367–7368.
13 S. J. Barrow, S. Kasera, M. J. Rowland, J. del Barrio and O. A. Scherman, *Chem. Rev.*, 2015, **115**, 12320–12406.
14 C. Klöck, R. N. Dsouza and W. M. Nau, *Org. Lett.*, 2009, **11**, 2595–2598.
15 K. I. Assaf and W. M. Nau, *Chem. Soc. Rev.*, 2015, **44**, 394–418.
16 B. Tang, J. Zhao, J.-F. Xu and X. Zhang, *Chem. – Eur. J.*, 2020, **26**, 15446–15460.
17 D. Li, Z. Feng, Y. Han, C. Chen, Q.-W. Zhang and Y. Tian, *Adv. Sci.*, 2022, **9**, 2104790.
18 X. Qiu, J. Seibert, O. Fuhr, F. Biedermann and S. Bräse, *Chem. Commun.*, 2024, **60**, 3267–3270.
19 S. Zhang, L. Zhang, A. Chen, Y. An, X.-M. Chen, H. Yang and Q. Li, *Angew. Chem., Int. Ed.*, 2024, e202410130.
20 A. Palma, M. Artelsmair, G. Wu, X. Lu, S. J. Barrow, N. Uddin, E. Rosta, E. Masson and O. A. Scherman, *Angew. Chem., Int. Ed.*, 2017, **56**, 15688–15692.
21 F. N. Tehrani, K. I. Assaf, R. Hein, C. M. E. Jensen, T. C. Nugent and W. M. Nau, *ACS Catal.*, 2022, **12**, 2261–2269.
22 K. de la Vega-Hernández, M. G. Suero and P. Ballester, *Chem. Sci.*, 2024, **15**, 8841–8849.
23 J. A. Finbloom, K. Han, C. C. Slack, A. L. Furst and M. B. Francis, *J. Am. Chem. Soc.*, 2017, **139**, 9691–9697.
24 T. G. Brevé, M. Filius, C. Araman, M. P. van der Helm, P.-L. Hagedoorn, C. Joo, S. I. van Kasteren and R. Eelkema, *Angew. Chem., Int. Ed.*, 2020, **59**, 9340–9344.
25 X. Feng, F. Zhao, R. Qian, M. Guo, J. Yang, R. Yang and D. Meng, *ChemistrySelect*, 2021, **6**, 10739–10745.
26 S. Moorthy, A. Castillo Bonillo, H. Lambert, E. Kalenius and T.-C. Lee, *Chem. Commun.*, 2022, **58**, 3617–3620.
27 N. Rad and V. Sashuk, *Chem. Sci.*, 2022, **13**, 12440–12444.
28 G. Li, Y. Wan, R. W. Lewis, B. Fan and R. Eelkema, *Cell Rep. Phys. Sci.*, 2023, **4**, 101309.
29 S. Mei, Q. Ou, X. Tang, J.-F. Xu and X. Zhang, *Org. Lett.*, 2023, **25**, 5291–5296.
30 S. Mkrtchyan, V. B. Purohit, S. Sarfaraz, M. Yar, K. Ayub and V. O. Iaroshenko, *ACS Sustainable Chem. Eng.*, 2023, **11**, 8406–8412.
31 X.-L. Li, K.-K. Niu, S. Yu, H. Liu and L.-B. Xing, *Chem. Commun.*, 2024, **60**, 8924–8927.
32 D. Liu, Y. Fan, M. Liu, Q. Ge, R. Gao and H. Cong, *Org. Lett.*, 2024, **26**, 3896–3900.
33 D. Majumder, S. Koley, A. Barik, P. Ruz, S. Banerjee, B. Viswanadh, N. Barooah, V. S. Tripathi, V. Sudarsan, A. Kumar, A. K. Tyagi, A. C. Bhasikuttan and J. Mohanty, *Nanoscale*, 2024, **16**, 10801–10811.
34 X. Tang, S. Mei, J.-F. Xu and X. Zhang, *Chem. Commun.*, 2024, **60**, 5286–5289.
35 S. Bräse, C. Gil, K. Knepper and V. Zimmermann, *Angew. Chem., Int. Ed.*, 2005, **44**, 5188–5240.
36 W. T. Borden, N. P. Gritsan, C. M. Hadad, W. L. Karney, C. R. Kemnitz and M. S. Platz, *Acc. Chem. Res.*, 2000, **33**, 765–771.
37 X. Qiu, Y. Wang, S. Leopold, S. Lebedkin, U. Schepers, M. M. Kappes, F. Biedermann and S. Bräse, *Small*, 2024, **20**, 2307318.
38 X. Qiu, E. Pohl, Q. Cai, J. Seibert, Y. Li, S. Leopold, O. Fuhr, M. A. R. Meier, U. Schepers and S. Bräse, *Adv. Funct. Mater.*, 2024, 2401938.
39 X. Qiu, T. Zheng, M. Runowski, P. Woźny, I. R. Martín, K. Soler-Carracedo, C. E. Piñero, S. Lebedkin, O. Fuhr and S. Bräse, *Adv. Funct. Mater.*, 2024, 2313517.
40 S. Sinn, E. Spuling, S. Bräse and F. Biedermann, *Chem. Sci.*, 2019, **10**, 6584–6593.
41 B. Luo and X. Song, *Eur. J. Med. Chem.*, 2021, **224**, 113688.